Proceedings of the 14th International Heat Transfer Conference
IHTC14
August 8-13, 2010, Washington, DC, USA

IHTC14-22989

Characterization of Carbon Nanotube Array based Thermal Interface Material after Bonding Process

Rong-Shiuan Chu
Applied Science and Technology Program
University of California
Berkeley, CA, USA

Yang Zhao
Department of Mechanical Engineering
University of California
Berkeley, CA, USA

Arun Majumdar
Director
Advanced Research Projects
Agency- Energy
US Department of Energy
Washington D.C., USA

Abstract

Vertically Aligned Carbon Nanotube (CNT) Arrays are promising to use as advanced thermal interface material. While possessing high thermal conductivity for an individual tube, carbon nanotube array based thermal interface materials (TIMs) fell short of expectations due to poor CNTs-target surface contacts. Investigations suggested that the overall resistance can be potentially reduced to less than 1 m^2-K/MW by increasing the number of tubes to target surface contacts. This paper use chromium/gold/indium assisted thermal pressure-bonding to enhance contacts. A CNT array with 12.7% areal density was bonded to an experimental glass surface with 2-μm indium bonding layer and 10 nm-chromium/150 nm-gold adhesion layers under pressure of 196 KPa and temperature of 350 ˚C. Phase sensitive photothermal reflectance method was used for thermal measurement. The overall resistance, including CNTs-glass contact resistance and effective CNT array thermal resistance, is 1.1 m^2-K/MW ± 27%. Although the contact resistance was reduced to 0.39 m^2-K/MW ± 15%, the effective thermal conductivity of the post-bonded 80 μm long CNTs was 114 W/m-K ± 22%, which was lower than the expected lower bound of the thermal conductivity of 12.7% filled CNT array. It was suggested that the deformation of CNT array after mechanical bonding reduced its performance.

Introduction

Increase of electronic device performance has been accompanied by increase of on chip power density. However, inadequate power dissipation, which results in increase of device operating temperature, will shorten device life time. Thermal Interface Materials (TIMs) are used to reduce thermal resistance at multiple-interfaces in the electronics. Two essential requirements for TIMs are high mechanical compliance to reduce contact resistance and high cross-plane thermal conductivity to ensure low volumetric resistance. Traditionally, TIMs are made of silicone based matrix loaded with high thermal conductivity particles. The lowest achievable resistance with such TIM is 2 m^2-K/MW [1], while the chip heat flux generated by high performance electronics is higher than 1 MW/m^2 and will be increasing more than 0.2 MW/m^2 annually [2]. Thus, TIM with resistance lower than 1 m^2-K/MW is needed.

Using CNT array bridging two mating surfaces is promising to reduce the overall resistance since it is compliant and was measured to have high thermal conductivity along axial direction for an individual CNT. The thermal conductivity for a single-wall CNT and a multiwall CNT are in the range of 2500-6600 W/m-K [3-6] and 2000-3000 W/m-K [7-8], respectively. However, investigations showed

that the overall resistance of CNT array based TIM fell short of expectations due to poor contacts between nanotube tips and target surfaces. Using 1-D steady heating system, Xu et al. [9] measured the overall resistance between two copper bars sandwitched with a 7-μm thick CNT array. The minimum overall resistance was found to be 19.8 m^2-K/MW under pressure of 440 KPa. Hu et al. [10] first extracted the contact resistance between CNTs and experimental surface by 3-omega method and found that the contact resistance dominated the overall resistance. The room temperature thermal conductivity of a 13-μm thick CNT array was measured to be 75 W/m-K. The contact resistance was measured to be 15.5 m^2-K/MW under pressure of 100 KPa, which was 2 orders of magnitude larger than the CNT array volumetric resistance. Tong et al. [11] reduced the contact resistance between a 7-μm thick CNT array and a glass surface by adding 1-μm thick indium film as bonding material. Using phase sensitive thermal reflectance method, the dry adhered contact resistance was measured to be 11 m^2-K/MW, while the indium assisted contact resistance was reduced to 0.29 m^2-K/MW.

In addition to the contact resistance, the thermal conductivity and the volumetric heat capacity of CNT array are also affected by the tubes-target surface contacts [12]. Panzer et al. [12] measured the effective thermal conductivity of a 28-μm thick, 12% filled CNT array to be 8 W/m-K by time domain thermal reflectance technique. The effective thermal conductivity was only 0.3% of the thermal conductivity of an individual CNT (~2500 W/m-K). The effective volumetric heat capacity of CNT array was also measured to be around 0.3% of the volumetric heat capacity. This was explained that the intertube thermal transport was negligible, and that the cross-plane thermal transport was contributed only by those tubes thermally contacted with target surfaces. Thus, the overall resistance can be potentially reduced to less than 1 m^2-K/MW by increasing the number of tubes-target surface contacts.

The use of pressure with indium contacts will most likely enhance the number of tubes contacting to the target surface. In this paper, we introduced a bonding technique with indium (In) bonding layer and chromium (Cr)/gold (Au) adhesion layer under pressure of 196 KPa and temperature of 350˚C to improve CNTs-target surface contacts. By constructing a three layer heat conduction model, we extracted the CNTs-target surface contact resistance, effective volumetric heat capacity and effective thermal conductivity of the CNT array from phase response measured by phase sensitive thermal reflectance method. The bonding effect on the thermal properties is discussed at the end.

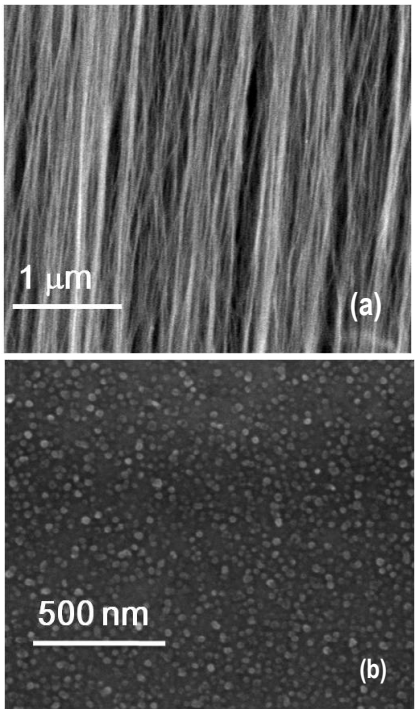

Fig. 1 (a) Cross-view SEM image of a vertically aligned CNT array. (b) Plan-view SEM image of the catalyst nanoparticles formed on substrate after CNTs growth. The CNTs were burned off by oxygen plasma.

Sample Preparation

The CNT array was grown on a silicon substrate through water assisted thermal chemical vapor deposition (CVD) process [13]. A 10 nm Aluminum Oxides (Al_2O_3) supporting layer was sputtered on the silicon substrate, followed by thermal evaporation of a 1 nm Iron (Fe) catalyst layer. The gases introduced during the thermal CVD process included argon, ethylene, hydrogen and water vapor. The growth temperature was 750˚C. Figure 1(a) shows a typical cross view of a vertically aligned CNT Array.

The tube density of the CNT array was determined from the SEM image. Figure 1(b) shows the plane-view SEM image of the catalyst nanoparticles formed on silicon substrate. The CNT array was initially grown on the substrate and burned off by oxygen plasma. The amorphous carbon was also burned off and left the bare nanoparticles on substrate. The nanoparticles were confirmed to be iron catalyst

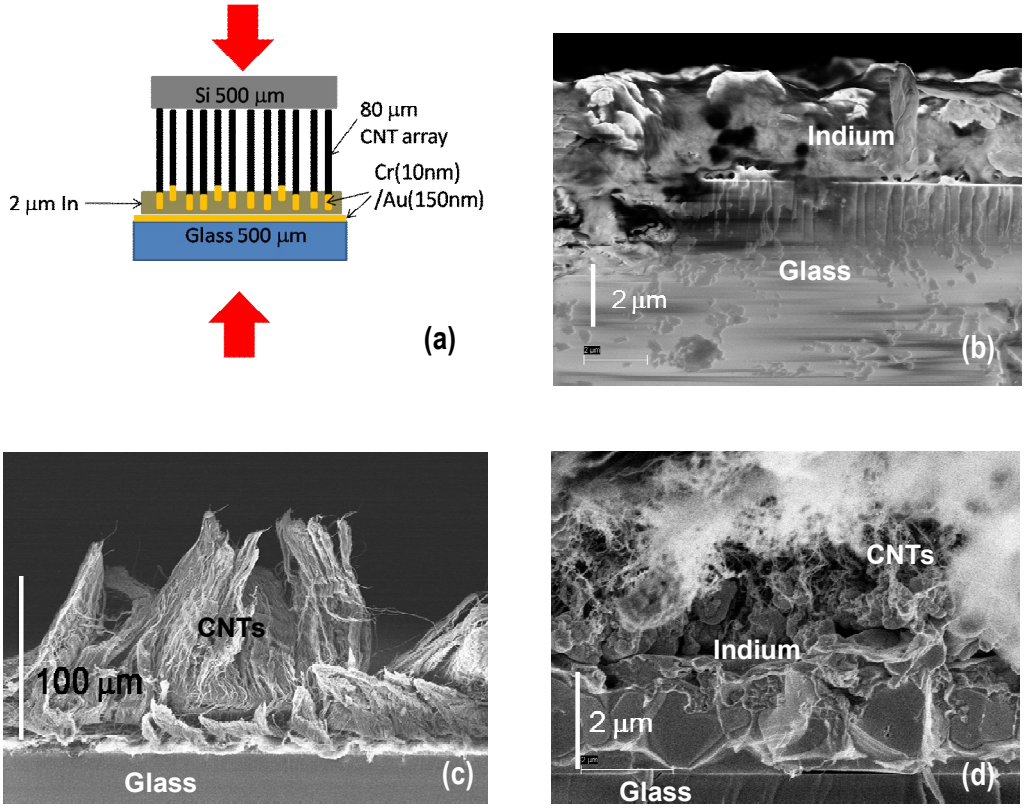

Fig. 2 (a) Schematic figure of a CNT array bonded on Cr/Au-coated side of glass with 2 μm indium as bonding layer and 10 nm chromium / 150 nm gold as adhesion layer. (b) Cross view SEM image at the interface between indium and Cr/Au-coated side of glass (c) Cross view SEM image of a CNT array after the bonding process. The silicon substrate was peeled off from the CNT array after Flipchip bonding process. (d) Cross view SEM image at the interface between indium and chromium/gold- deposited CNT array.

by returning the oxygen plasma etched substrate to CVD process which had CNTs growth afterwards. By counting all the nanoparticles in the field of view of the SEM image, we measured particles density to be 8 x 10^{10} particles/cm^2. In figure 1(a), the diameter of the tube was estimated to be 20 nm, which is close to the diameter of the catalyst nanoparticles shown in the SEM image of 1(b). The tubes density was estimated to be 50% of the catalyst density by peeling off the CNT array from the silicon substrate and counting the ratio of CNTs uprooted holes to amorphous coverage nanoparticles on the silicon substrate in the field of view of the SEM picture. The detail measurement on catalyst activation rate and the SEM picture of CNTs uprooted holes will be reported in follow-up paper. With tube number density and tube diameter, we estimated the areal density of the CNT array on the substrate to be 12.7%, and thus the volume fraction of CNT array is 12.7%.

Another piece of CNT array with same growing condition was bonded to a 500 μm tick glass used as target contact surface by flipchip bonding technique shown in the schematic figure 2(a). The bonding pressure was 196 KPa, and it was withholding for 10 minutes at temperature of 350 ˚C. Cr (10nm)/Au (150nm) films were sequentially sputtered on both CNT array surface and glass surface as adhesion layer. A 2 μm thick indium was thermally evaporated on glass as bonding layer. To simplify sample structure for modeling, the silicon substrate was removed from the CNT array after bonding. The post-bonded CNT array was around 80 μm long measured under optical microscope. The indium was melted and deformed during the bonding process which has thickness about 2 μm after solidified as shown in figure 2 (b). Figure 2 (c) shows a typical cross view SEM image of a post-bonded CNT array under the same bonding process. The CNT array was deformed and non-vertically aligned. The image of the In-Cr/Au-coated CNTs interface (figure 2 (d)) indicates that the indium melted and filled between tubes during the bonding process while formed non-uniform micron-large clusters after solidified. The bonding effect on the thermal properties, including CNTs-glass surface contact

resistance, effective volumetric heat capacity and effective thermal conductivity of CNT array, is verified in the following sections.

Measurement Principles

The frequency domain thermal reflectance technique is completed by a modulated continuous wave diode laser as heating source, a low power He-Ne laser as probe beam, and a photo diode to detect intensity change in the reflected probe beam. The reflectance modulation is due to temperature dependence of refractive index. The experimental set up is shown in figure 3 (a). A function generator sends a modulation signal to the driver of pump laser. The pump laser is a 3 W continuous wave diode laser with nominal wave length 808 nm. In figure 3 (b), the pump beam goes through glass and absorbed at the Cr/Au layer coated on glass with heating diameter to be 1 mm. By periodically heating the sample, the temperature at the Cr/Au surface is oscillating at modulation frequency ω. A low power (~5mW) He-Ne probe laser with wave length 633 nm goes through glass and concentrically aligned with pump beam at the Cr/Au surface. Since pump and probe beam are focused at the Cr/Au surface, the Cr/Au layer are used as both reflectance thermometry and absorption layer. The intensity of the reflected probe beam oscillates at frequency ω due to temperature dependence of the refractive index. The band pass filter in front of photodiode is used to filter out the pump beam. The signal (amplitude and phase) of the temperature oscillation is obtained by using Lock-In Amplifier with the modulation signal as reference.

In figure 3 (c), the intensities of pump and probe beam represent the periodic input heat source and oscillation of Cr/Au surface temperature. The oscillation of the intensity of reflected probe beam has a phase lag φ with respect to the pump beam. This phase lag depends only on the thermal properties of the sample and modulation frequency.

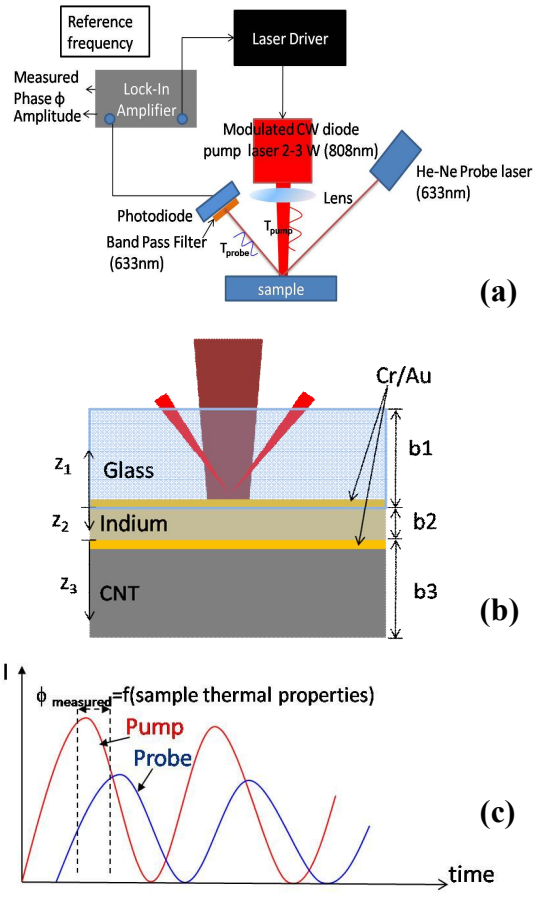

Fig. 3 Schematic (a) experimental Setup for Phase Sensitive Thermal Reflectance Technique (b) sample geometry and heat conduction model (c) diagram of pump and probe beam as thermal waves.

Heat Conduction Model

The thermal properties are extracted from the heat conduction model by using the model phase fit to the experimental phase response. A three layer heat conduction model is shown in figure 3 (b). The Cr/Au coated glass, indium, and the CNT array are the first, second and third layer respectively, and z_j, b_j are the cross-plane coordinate and effective thickness at the j^{th} layer.

A periodic heat source with power Q and heating radius a is absorbed at z_1=0. It is assumed that no heat loss to the surrounding, and no boundaries along in-plane (r) direction. The three-layer heat conduction equation in cylindrical coordinates and boundary conditions are

$$\frac{C_j}{k_j}\frac{\partial T_j(r,z,t)}{\partial t} = n_j \frac{1}{r}\frac{\partial}{\partial r}\left(r\frac{\partial T_j(r,z,t)}{\partial r}\right) + \frac{\partial^2 T_j(r,z,t)}{\partial z_j^{\,2}}$$

$$\frac{Q}{\pi a^2} e^{-i\omega t} = -k_1 \left.\frac{\partial T_1}{\partial z_1}\right|_{z_1=0} + (R_{1-2})^{-1}(T_1(0) - T_2(0))$$

$$k_2 \left.\frac{\partial T_2}{\partial z_2}\right|_{z_2=0} = (R_{1-2})^{-1}(T_2(0) - T_1(0))$$

$$k_2 \left.\frac{\partial T_2}{\partial z_2}\right|_{z_2=b_2} = (R_{2-3})^{-1}(T_2(0) - T_3(0)) = k_3 \left.\frac{\partial T_3}{\partial z_3}\right|_{z_3=0}$$

$$\left.\frac{\partial T_1}{\partial z_1}\right|_{z_1=b_1} = 0; \quad \left.\frac{\partial T_3}{\partial z_3}\right|_{z_3=b_3} = 0 \qquad (1)$$

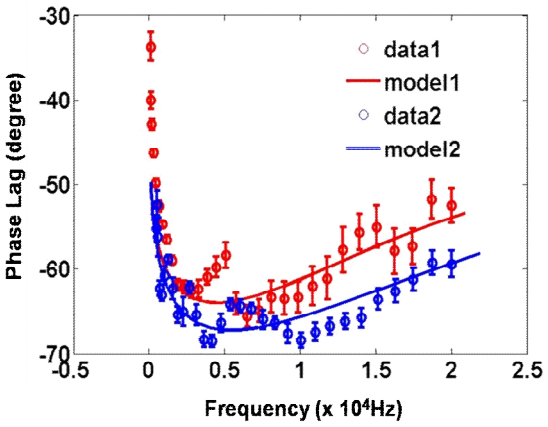

Fig. 4 Experimental phase response for the two measurements of the 80-μm long CNT sample and the model calculated phase versus modulation frequency. The two measurements at different locations on the sample were individually fitted by the model phase.

where T_j, C_j, k_j, and n_j are the temperature distribution, effective volumetric heat capacity, effective cross-plane thermal conductivity, and thermal conductivity anisotropic ratio, of j^{th} material respectively. $R_{1\text{-}2}$ is the contact resistance between indium and Au-coated side of glass and $R_{2\text{-}3}$ is the contact resistance between CNT array and indium.

The fixed parameters include properties (C, k, b, and n) of glass and indium, the effective thickness of CNT array (b_3), and the contact resistance between Au coated side glass and indium ($R_{1\text{-}2}$). Since the indium film was thermally evaporated on the Au-coated side of glass surface, the as-deposited metal-metal contact resistance is of order of 1 m^2-K/GW [14]. The fitting parameters are $R_{2\text{-}3}$, k_3, n_3, and C_3. The effective volumetric heat capacity of CNT array, C_3, is expressed as

$$C_3 = C_{CNT} \times \rho_{CNT} \times f_{C,effecitve} \quad (2)$$

where the heat capacity of an individual CNT, C_{CNT}, is 660 J/kg-K [15], and the density of an individual CNT, ρ_{CNT}, is 1330 kg/m^3 [13]. The effective volume fraction of the CNT array contributing to the heat capacity, $f_{C,effective}$, is related to the number of tubes thermally contact with the target surface, which is difficult to determined by direct observation. Using Integral Transform method [11], the temperature distribution at the Cr/Au-coated glass surface is numerically solved as a complex number, and its phase is the polar angle of the complex numbers. The best fit solutions to the experimental phase response are solved through least square multi-parameter searching process.

Results and Discussions

Figure 4 shows two experimental phase responses measured at different location on the sample along with their least square best-fit solutions versus modulation frequency. The phase response varies with modulation frequency from 100 Hz to 20000 Hz. The best fit solutions with uncertainties of the fitting parameters from the two measurements and their averaged results are listed in table 1. The uncertainty of each fitting parameter is the percentage of variation around its best fit value allowed by the measurement error represented by the error bars in Fig. 4.

The averaged best fit value in table 1 shows that the effective volumetric heat capacity is 110.6 KJ/m^3-K, which has an effective volume fraction ($f_{C,\ effective}$), 12.6%, if the heat capacity of

Table 1 Best-fit values with uncertainties of indium-CNT array contact resistance $R_{2\text{-}3}$, effective CNT array cross-plane thermal conductivity k_3, effective CNT array volumetric heat capacity C_3, and CNT array anisotropic ratio n_3 from the two measurements of the 80 μm long CNT array sample.

	Point 1	Point 2	**Average**
$R_{2\text{-}3}$ (m^2-K/MW)	0.31 ± 13%	0.48 ± 16%	**0.39 ± 15%**
k_3 (W/m-K)	125 ± 20%	103 ± 23%	**114 ± 22%**
C_3 (kJ/m^3-K)	111.5 ± 10%	109.7 ± 11%	**110.6 ± 11%**
n_3	<0.1	<0.1	**<0.1**

an individual CNT is 660 J/kg-K [15] and the density of an individual CNT is 1330 kg/m^3 [13]. The effective volume fraction is close to the true volume fraction of CNT array and much larger than the effective volume fraction (~0.3%) of the 10% filled 160nm-Aluminum/20nm-Palladium -deposited CNT array [12]. This suggests that the bonding improved the tubes-target surface contacts.

Assume that the intertube coupling is negligible if the spacing between tubes was greater than 1.3 nm [16], the effective volume fraction contributing to the conduction and contact resistance ($f_{R,effective}$) is the same as the effective volume fraction contributing to the volumetric heat capacity of CNT array [12].

$$f_{R,effective}=f_{C,effective}= 12.6\% \quad (3)$$

Since the best fit averaged indium-CNT array contact resistance, $R_{2\text{-}3}$, is measured to be 0.39 m^2-K/MW, the indium-individual CNT contact resistance is 49 m^2-K/GW by scaling a factor of 12.6%. A femto-second pump probe system measured the Cr-Graphite contact resistance to be around 20 m^2-K/GW (internal discussion with Pamela M. Norris group, Department of Mechanical and Aerospace Engineering, University of Virginia). The Cr-individual CNT contact resistance can be estimated to be 20 m^2-K/GW since an individual CNT has a qusi-2D surface area. The Cr-Au contact resistance is estimated to be about 1 m^2-K/GW by using the contact resistance of flat metal-metal surface [14], then the In-Au contact resistance is 28 m^2-K/GW since the Cr-CNT, Cr-Au, and In-Au contact resistances are in-series. The In-Au contact resistance is an order of magnitude larger than the usual flat metal-metal contacts [14], which shows that the wetting of In to Cr/Au coated tube is not good.

Table 1 shows that the thermal conductivity anisotropic ratio (n_3) has a upper bound of 0.1, and the averaged effective thermal conductivity of CNT array, 114 W/m-K, was 4.6% of the thermal conductivity of an individual multiwall CNT (~2500 W/m-K). This is lower than the expected effective fraction (12.6%) contributing to the conduction. It can be explained by the deformation of the CNT arrays during mechanical bonding. The non-vertically aligned and deformed CNT array forms multiple CNT junctions connected by vander waals force within CNT film. Such weak bonding at the junctions creates large contact resistance (> 0.1 m^2-K/MW) [16] which reduced the performance of cross-plane thermal transport. The thermal resistance of the 80 μm thick CNT array is 0.7 m^2-K/MW, and the overall resistance, including In-CNT array contact resistance and the thermal resistance of CNT array, is around 1.1 m^2-K/MW.

Conclusions

In this work, we studied the thermal properties of CNT array after In-assisted bonding process. The CNT array was attached to a glass surface with 1-μm indium as bonding layer and 10-nm Chromium/ 150-nm gold as adhesion layer under pressure of 196 KPa and temperature of 350°C. The CNT array was deformed and the indium layer formed to micron-large clusters within CNT array. Phase sensitive thermal reflectance technique was used for thermal properties measurement. Results showed that the effective volume fraction contributing to the thermal transport (12.6%) is close to the true volume fraction of CNT array. This suggests that the bonding improved the tubes-target surface contacts. With improved contact at the interface, the overall thermal resistance reaches 1.1 m^2-K/MW. The thermal conductivity of the CNT array was measured to be 114 W/m-K, which was only 4.6% of the thermal conductivity of an individual multiwall CNT. This could be due to the degradation of thermal transport from the deformed CNT array. Therefore, preserving the vertically aligned structure of CNT arrays during the bonding process is important to further improve the thermal performance of the CNT array based TIMs.

Nomenclature

a	radius of heating laser spot, m
b	thickness, m
C	heat capacity, J/kg-K
C_v	volumetric heat capacity, kJ/m^3-K
f_a	area fraction
f_v	volume fraction
k	thermal conductivity, W/m-K
Q	absorbed power, W
R	interface thermal resistance, m^2-K/MW
r	radial coordinate, m
T	temperature distribution function, K
t	time, s
z	cross-plane coordinate, m
φ	phase lag, degree
ρ	density, kg/m^3
ω	modulation frequency, Hz

Subscripts

1 glass layer
2 indium layer
3 CNT array layer
j j^{th} material

Acknowledgments

We thank Dr. Pamela M. Norris, Justin L. Smoyer and John C. Duda in Department of Mechanical and Aerospace Engineering, University of Virginia for measuring the contact resistance between chromium and graphite. We thank Dr. David J. Hwang and Dr. Costas P. Grigoropoulos in Department of Mechanical Engineering, University of California, Berkeley, for providing the facility of high resolution SEM and taking the SEM image of catalyst nanoparticles. We thank Dr. Oscar Dubon in Department of Material Science Engineering for giving advice in this work. This work is supported by Office of Naval Research (*ONR*) Multidisciplinary University Research Initiative (*MURI*) program. We thank Molecular Foundry in Lawrence Berkeley National Laboratory (*LBNL*) and UC Berkeley Microlab for providing facilities used in this work.

References

1. Prasher, R.S., 2006, "Thermal Interface Materials: Historical Perspective, Status, and Future Direction," Proceedings of the IEEE, 94(8), pp. 1571-1586.
2. Anandan, S.S., and Ramalingam, V., 2008, "Thermal Management of Electronics: a Review of Literature," Thermal Science, 12(2), pp. 5-26.
3. Osman, M.A., and Srivastava, D., 2001, "Temperature Dependence of the Thermal Conductivity of Single-Wall Carbon Nanotubes," Nanotechnology 12(1), pp.21-24.
4. Berber, S., Kwon, Y.-K., and Tomanek, D., 2000, "Unusually High Thermal Conductivity of Carbon Nanotubes," Phys. Rev. Lett. 84(20), pp.4613-4616.
5. Maruyama, S., 2003, "A Molecular Dynamics Simulation of Heat Conduction Of a Finite Length Single-Walled Carbon Nanotube," Microscale Thermophys Eng., 7(1), pp.41-50.
6. Pop, E., Mann, D., Wang, Q., Goodson, K., and Dai, H., 2006, "Thermal Conductance of an Individual Single-Wall Carbon Nanotube above Room Temperature," Nano Lett. 6(1), pp.96-100.
7. Kim, P., Shi, L., Majumdar, A., and McEuen, P.L., 2001, "Thermal Transport Measurements of Individual Multiwalled Nanotubes," Phys. Rev. Lett., 87(21), pp. 215502.
8. Fujii, M., Zhang, X., Xie, H., Ago, H., Takahashi, K., Ikuta, T., Abe, H., and Shimizu, T., 2005, "Measuring the Thermal Conductivity of a Single Carbon Nanotube," Phys. Rev. Lett. 95(6), pp. 065502.
9. Xu, J. and Fisher, T.S., 2006, "Enhanced thermal contact conductance with carbon nanotube arrays," International Journal of Heat and Mass Transfer vol. 49, pp. 1658-1666.
10. Hu, X.J., Padilla, A.A., Xu, J., Fisher, T.S., Goodson, K.E., 2006, "3-Omega Measurements of Vertically Oriented Carbon Nanotubes on Silicon," ASME J. Heat Transfer, 128(11), pp. 1109-1113.
11. Tong, T., Zhao, Y., Delzeit, L., Kashani, A., Meyyappan, M., and A. Majumdar, 2007, "Dense Vertically Aligned Multiwalled Carbon Nanotube Arrays as Thermal Interface Materials," IEEE Transactions on Components and Packaging Technologies, Vol. 30, pp. 92-101.
12. Panzer, M.A., Zhang, G., D., Mann, Hu, X., Pop, E., Dai, H., and Goodson, K.E., 2008, "Thermal properties of Metal-Coated Vertically Aligned Single-Wall Nanotube Arrays," Journal of heat Transfer, vol. 130, pp.052404-1-052401-9.
13. Futaba, D.N., Hata, K., Namai, T., Yamada, T., Mizuno, K., Hayamizu, Y., Yumura, M., and Iijima, S., 2006, "84% Catalyst Activity of Water-Assisted Growth of Single Walled Carbon Nanotube Forrest Characterization by a Statistical and Macroscopic Approach," J. Phys. Chem. B, 110, pp. 8035-8038.
14. Gundrum, B.C., Cahill, D.G., and Averback, R.S., 2005, "Thermal Conductance of Metal-Metal Interfaces," Phys. Rev. B., 72(24), pp. 245426-1-5.
15. Hone, J., Batlogg, B., Benes, Z., Johnson, A. T., and Fischer, J. E., 2000, "Quantized Phonon Spectrum of Single-Wall Carbon Nanotubes," Science, 298(5485), pp. 1730-1733.
16. Zhong, H., and Lukes, J. R., 2006, "Interfacial Thermal Resistance Between Carbon Nanotubes: Molecular Dynamics Simulations and Analytical Thermal Modeling," Phys. Rev. B 74(12), pp.125403-1-125403-10.